

Biological and physicochemical properties of bovine sodium caseinate hydrolysates obtained by a bacterial protease preparation



María Eugenia Hidalgo^{a, b, *}, Ana Paula Folmer Côrrea^c, Manuel Mancilla Canales^{a, b}, Daniel Joner Daroit^d, Adriano Brandelli^c, Patricia Risso^{a, b, e}

^a Departamento de Química-Física, Facultad de Ciencias Bioquímicas y Farmacéuticas, Universidad Nacional de Rosario (UNR), Suipacha 531, 2000 Rosario, Santa Fe, Argentina

^b Instituto de Física Rosario (IFIR-CONICET-UNR), 27 de Febrero 210 Bis, 2000 Rosario, Santa Fe, Argentina

^c Instituto de Ciência e Tecnologia de Alimentos (ICTA), Universidade Federal de Rio Grande do Sul (UFRGS), Av. Bento Gonçalves 9500, 91501-970 Porto Alegre, Brazil

^d Universidade Federal da Fronteira Sul (UFFS), Campus Cerro Largo, 97900-000 Cerro Largo, RS, Brazil

^e Facultad de Ciencias Veterinarias, Universidad Nacional de Rosario (UNR), Ovidio Lagos y Ruta 33 2170 Casilda, Santa Fe, Argentina

ARTICLE INFO

Article history:

Received 22 October 2013

Accepted 7 July 2014

Available online 31 July 2014

Keywords:

Bacillus sp.P7

Bovine sodium caseinate

Hydrolysates

Bioactivity

Acid aggregation and gelation

Microstructure

ABSTRACT

In this work, we aimed at the production of bovine sodium caseinate (NaCAS) hydrolysates by means of an extracellular protease from *Bacillus* sp. P7. Mass spectrometry was carried out to evaluate peptide mass distribution and identified sequences of peptides with a signal/noise ratio higher than 10. Antioxidant and antimicrobial properties of hydrolysates were evaluated. An acid-induced aggregation process of the hydrolysates and their corresponding mixtures with NaCAS were also analyzed. The results showed that the enzymatic hydrolysis produced peptides, mostly lower than 3 kDa, with different bioactivities depending on the time of hydrolysis (t_i). These hydrolysates lost their ability to aggregate by addition of glucono- δ -lactone, and their incorporation into NaCAS solutions alter the kinetics of the process. Also, the degree of compactness of the NaCAS aggregates, estimated by the fractal dimension of aggregates, was not significantly altered by the incorporation of hydrolysates. However, at higher protein concentrations, when the decrease in pH leads to the formation of NaCAS acid gels, the presence of hydrolysates alters the microstructure and rheological behavior of these gels.

© 2014 Elsevier Ltd. All rights reserved.

1. Introduction

Caseins (CN) are the main milk protein fraction (~80%) which occurs in micelles as large particles of colloidal size (Walstra, Jenness, & Badings, 1984). However, the micellar structure of CN is destroyed during the manufacture of sodium caseinate (NaCAS) (Mulvihill & Fox, 1989). NaCAS are extensively used in food industry because of their physicochemical, nutritional and functional properties, such as emulsifying and gelation capacities, thus contributing to food texture (Alvarez, Risso, Gatti, Burgos, & Suarez Sala, 2007; Nishinari, Zhang, & Ikeda, 2000).

A gel structure is formed during NaCAS acidification as a result of the dissociation and aggregation of CN fractions (α_{S1} -, α_{S2} -, β - and

κ -). In the traditional process, NaCAS is acidified by bacteria which ferment lactose to lactic acid. However, direct acidification achieved by the addition of a lactone, such as glucono- δ -lactone (GDL), has gained the attention of the food industry, since this process avoids potential complications related to starter bacteria (variable activity and variations with the type of culture used). In fact, the final pH of the system bears a direct relation to the amount of GDL added, whereas starter bacteria produce acid until they inhibit their own growth as pH becomes lower (Braga, Menossi, & Cunha, 2006; de Kruif, 1997).

The high growth in consumer demand for healthy and nutritional food products has encouraged the food industry to carry out an improvement in the development of natural and functional food ingredients and dietary supplements. In the primary sequence of proteins there are inactive peptides that could be released by enzymatic hydrolysis *in vivo* or *in vitro*. These peptides acquire different biological activities, such as opioid, antihypertensive, immunomodulatory, antibacterial and antioxidant activities, among others, with potential applications in food science and

* Corresponding author. Departamento de Química-Física, Facultad de Ciencias Bioquímicas y Farmacéuticas, Universidad Nacional de Rosario (UNR), Suipacha 531, 2000 Rosario, Santa Fe, Argentina.

E-mail addresses: maruhidalgo80@yahoo.com.ar, mhidalgo@conicet.gov.ar (M.E. Hidalgo).

technology (FitzGerald, Murray, & Walsh, 2004; Haque & Chand, 2008; Phelan, Aherne, FitzGerald, & O'Brien, 2009; Sarmadi & Ismail, 2010; Silva & Malcata, 2005).

CN are considered important sources of bioactive peptides that could be released through different types of enzymatic hydrolysis using microbial or digestive enzymes (Korhonen, 2009; Silva & Malcata, 2005). Under moderate conditions of pH and temperature, it is possible to obtain components with biological activities that enhanced nutritional and functional properties such as gelation, emulsification and foam formation (Hartmann & Meisel, 2007; Silva & Malcata, 2005).

It is known that commercial proteases have been employed in the production of protein hydrolysates with bioactive properties such as antioxidant activity (Rival, Boeriu, & Wichers, 2001; Saiga, Tanabe, & Nishimiura, 2003; Zhu, Zhou, & Qian, 2006). Microbial proteases are particularly interesting because of the high yield achieved during their production through well-established culture methods (Gupta, Beg, & Lorenz, 2002; Rao, Tanksale, Ghatge, & Deshpande, 1998). It has been reported that a proteolytic *Bacillus* sp. P7, isolated from the intestinal conduct of the Amazonian fish *Piaractus mesopotamicus*, produces high levels of extracellular proteases with biotechnological potential during submerged cultivations in inexpensive culture media (Corrêa et al., 2011).

Enzymatic hydrolysis of proteins might be an alternative treatment to control the characteristics of acid-set gels and to confer desired rheological and organoleptic properties (Rabiey & Britten, 2009). The aims of this work were to obtain protein hydrolysates of bovine NaCAS with a protease preparation from *Bacillus* sp. P7, determine the peptide mass distribution, identified peptide sequences and evaluate their different bioactivities (antioxidant, antimicrobial, reducing and chelating power). Also, the effects of the presence of these bioactive peptides on acid aggregation and gelation properties of NaCAS were studied.

2. Materials and methods

2.1. Materials

Bovine NaCAS powder, azocasein, the acidulant GDL, tris(hydroxymethyl)aminomethane (Tris), 8-anilino-1-naphthalene-sulfonate (ANS) as ammonium salt; 2,4,6-trinitrobenzene sulfonic acid (TNBS); 2,2'-azino-bis-(3-ethylbenzothiazoline)-6-sulfonic acid (ABTS); ferrozine (3-(2-pyridyl)-5,6-bis(4-phenyl-sulfonic acid)-1,2,4-triazine) were commercially acquired from Sigma-Aldrich Co. (Steinheim, Germany). Other chemicals employed were of analytical grade and were provided by Cicarelli SRL (San Lorenzo, Argentina).

2.2. Bovine sodium caseinate (NaCAS) preparation

NaCAS solutions were prepared by dissolving the commercial powder in distilled water. CN concentration was measured according to the Kuaye's method, which is based on the ability of strong alkaline solutions (0.25 mol L⁻¹ NaOH) to shift the spectrum of the amino acid tyrosine to higher wavelength values in the UV region (Kuaye, 1994). All the values obtained were the average of two determinations.

2.3. Microorganism and protease preparation

Bacillus sp. P7, which secretes the extracellular proteases, was maintained in Brain-Heart Infusion (BHI) agar plates. The strain was cultivated in feather meal broth (10 g L⁻¹ feather meal, 0.3 g L⁻¹ Na₂HPO₄, 0.4 g L⁻¹ NaH₂PO₄, 0.5 g L⁻¹ NaCl) for 48 h at 30 °C in a rotary shaker (125 rpm) (Corrêa, Daroit, & Brandelli, 2010). Culture

was centrifuged (10,000 × g for 15 min at 4 °C) and the supernatant, which contained the extracellular proteolytic enzymes, was submitted to a partial purification.

2.4. Protease partial purification

The proteases were precipitated from culture supernatants by the gradual addition of solid ammonium sulfate to achieve 60% saturation, in an ice bath with gentle stirring. This mixture was allowed to stand for 1 h, centrifuged (10,000 × g for 15 min at 4 °C), and the resulting pellet was dissolved in 20 × 10⁻³ mol L⁻¹ Tris-HCl buffer pH 8.0. The concentrated enzyme samples were applied to a Sephadex G-100 (Pharmacia Biotech, Uppsala, Sweden) gel filtration column (25 × 0.5 cm) previously equilibrated with the above mentioned buffer, and elution was performed using the same buffer at a flow rate of 0.33 mL min⁻¹. Thirty fractions (1 mL) were collected and submitted to the proteolytic activity assay. Fractions showing enzymatic activity were pooled to will be use in NaCAS hydrolysis.

2.5. Proteolytic activity assay

Proteolytic activity was determined as described by Corzo-Martínez, Moreno, Villamiel and Harte (2010), using azocasein as substrate. The reaction mixture contained 100 µL enzyme preparation, 100 µL of 20 × 10⁻³ mol L⁻¹ Tris-HCl buffer pH 8.0, and 100 µL of 10 mg mL⁻¹ azocasein in the same buffer. The mixture was incubated at 37 °C for 30 min, and the reaction was stopped by adding 500 µL of 0.10 g mL⁻¹ trichloroacetic acid (TCA). After centrifugation (10,000 × g for 5 min), 800 µL of the supernatant was mixed with 200 µL of 1.8 mol L⁻¹ NaOH, and the absorbance at 420 nm was measured (Corzo-Martínez et al., 2010). One unit of enzyme activity (U) was considered as the amount of enzyme that caused a change of 0.1 absorbance units under the above assay conditions. Fractions showing proteolytic activity on azocasein were pooled and employed as a P7 protease preparation (P7PP) for NaCAS hydrolysis.

2.6. Hydrolysis of NaCAS

Samples of 0.01 g mL⁻¹ of NaCAS in Tris-HCl buffer 20 × 10⁻³ mol L⁻¹, pH 8 were subjected to hydrolysis with the addition of 1 mL of P7PP (enzyme:substrate 1:50 ratio) at 45 °C. The hydrolysis reaction was stopped at different times (*t*; *i* = 0, 0.5, 1, 2, 3, 4, 6 and 7 h) by heating the samples to 100 °C for 15 min. After centrifugation (10,000 × g for 15 min), the supernatants were recovered, lyophilized, and kept at -18 °C. Protein concentration of the supernatants was measured as previously described (Kuaye, 1994).

2.7. Degree of hydrolysis (DH)

DH of NaCAS hydrolysates was determined by the TNBS method (Adler-Nissen, 1979). Protein hydrolysate samples (250 µL) were mixed with 2 mL phosphate buffer (0.212 mol L⁻¹; pH 8.2) and 2 mL 1% TNBS, and incubated at 50 °C for 1 h. Then, 4 mL of 0.1 mol L⁻¹ HCl was added, and mixtures were maintained for 30 min at room temperature before performing readings at 340 nm. Total amino groups in NaCAS was determined in a sample (10 mg) which was completely hydrolyzed in 4 mL of 6 mol L⁻¹ HCl at 110 °C for 24 h (Li, Chen, Wang, Ji, & Wu, 2007).

2.8. Mass spectrometry

Peptide mass distribution of hydrolysates was determined by MALDI-TOF-TOF mass spectrometry, at the CEQUIBIEM proteomic

facility from the Universidad de Buenos Aires, using an Ultraflex II mass spectrometer (Bruker Corporation, USA). Peaks with a signal/noise ratio higher than 10 were fragmented. The peptide sequences were predicted from the MS/MS data by using the proteomic tool Protein Prospector v.5.12.1 (<http://prospector.ucsf.edu/prospector/mshome.htm>) with the following searching conditions: NCBI 2013.6.17, taxonomy: *Bos taurus*, digestion: no enzyme, 200 ppm for parent ion tolerance, and 300 ppm for ion fragment tolerance.

2.9. Intrinsic fluorescence spectra

Excitation and emission spectra of the hydrolysates (1 mg mL⁻¹) were obtained to detect any spectral shift and/or changes in the relative intensity of fluorescence (FI) in an Aminco Bowman Series 2 spectrofluorometer (Thermo Fisher Scientific, USA). The excitation wavelength (λ_{exc}) and the range of concentration with a negligible internal filter effect were previously determined. For spectral analysis and FI measurements samples (3 mL) were poured into a fluorescence cuvette (1 cm light path) and placed into a cuvette holder maintained at 35 °C. Values of FI ($n = 2$) were registered within the range of 300–420 nm using a λ_{exc} of 286 nm.

2.10. Surface hydrophobicity (S_0)

S_0 was estimated according to Kato and Nakai method (Kato & Nakai, 1980), using the ammonium salt of amphiphilic ANS as a fluorescent probe. The measurements were carried out using λ_{exc} and emission wavelength (λ_{em}) set at 396 and 489 nm, respectively, at a constant temperature of 35 °C. Both wavelengths were previously obtained from emission and excitation spectra of protein-ANS mixtures.

Intensity of fluorescence of samples containing ANS and different concentrations of NaCAS hydrolysates (FI_b) as well as the intrinsic FI without ANS (FI_p) were determined ($n = 3$). The difference between FI_b and FI_p (ΔF) was calculated, and S_0 was determined as the initial slope in the ΔF vs. protein concentration (g mL⁻¹) plot.

2.11. NaCAS hydrolysates bioactivities in vitro

2.11.1. Antioxidant activity: ABTS method

Scavenging of the ABTS radical was determined by the decolorization assay described by Re et al. (1999). ABTS radical cation (ABTS⁺) solution was prepared by reacting 7×10^{-3} mol L⁻¹ ABTS solution with 140×10^{-3} mol L⁻¹ K₂SO₄ (final concentration). This mixture was allowed to stand in the dark at room temperature for 12–16 h before use. For the assay, the ABTS⁺ solution was diluted with 5×10^{-3} mol L⁻¹ phosphate buffered saline pH 7.0 (PBS) to an absorbance of 0.70 ± 0.02 at 734 nm. A 10 μ L (15 mg mL⁻¹) of sample was mixed with 1 mL of diluted ABTS⁺ solution and absorbance at 734 nm was measured after 6 min. Trolox[®] was used as a reference standard. The percentage inhibition of absorbance at 734 nm was calculated and plotted as a function of the concentration of the reference antioxidant (Trolox[®]) (Re et al., 1999).

2.11.2. Metal chelating activity

The chelating activity of Fe²⁺ was measured using the method described by Chang, Wu, and Chiang (2007), with slight modifications. One milliliter of sample (3.5 mg mL⁻¹) was mixed with 3.7 mL distilled water and then the mixture was reacted with 0.1 mL of 2×10^{-3} mol L⁻¹ FeSO₄ (Fe²⁺) and 0.2 mL of 5×10^{-3} mol L⁻¹ ferrozine. After 10 min, the absorbance was read at 562 nm. One milliliter of distilled water, instead of sample, was used as a control. Ethylene diamine tetra acetic acid (EDTA) 20 mg mL⁻¹ was used as standard (Chang et al., 2007). The results were expressed

as Chelating activity (%) = $[1 - (A/A_0)] \cdot 100$, where A is the absorbance of the test and A_0 is the absorbance of the control.

2.11.3. Reducing power

Reducing power of the hydrolysates was measured as previously described by Zhu et al. (2006). Samples (15 mg mL⁻¹) from each hydrolysis period were mixed with 2.5 mL phosphate buffer 0.2 mol L⁻¹ pH 6.6 and 2.5 mL potassium ferricyanide (10 mg mL⁻¹), and then the mixture was incubated at 50 °C for 20 min. Then, 2.5 mL TCA (0.10 g mL⁻¹) was added and the mixture was centrifuged (3000 \times g for 10 min). One milliliter of supernatant was mixed with 2.5 mL distilled water and 0.2 mL ferric chloride (1 mg mL⁻¹), and the absorbance at 700 nm was measured. Higher absorbance of the reaction mixture indicated greater reducing power. Butylatedhydroxytoluene (BHT) at the same concentration of samples was used as a positive control (Zhu et al., 2006).

2.11.4. Antibacterial activity

Antibacterial activity was determined according to Motta and Brandelli (2002) with modifications. The indicator strains tested were *Listeria monocytogenes* ATCC 15131, *Bacillus cereus* ATCC 9634, *Corynebacterium fimi* NCTC 7547, *Staphylococcus aureus* ATCC 1901, *Salmonella* Enteritidis ATCC 13076, and *Escherichia coli* ATCC 8739. Indicator microorganisms, at a concentration of 10^8 CFU mL⁻¹ in saline solution (NaCl 0.0085 g mL⁻¹), were inoculated with a swab onto BHI agar plates. Aliquots of 15 μ L NaCAS hydrolysates (250 mg mL⁻¹) were spotted on the freshly prepared lawn of indicator strain, and plates were incubated at the optimal temperature for each test microorganism. Subsequently, zones of growth inhibition represented by clear haloes were measured and presented as inhibition zone (mm) (Motta & Brandelli, 2002).

2.12. Determination of size variations of particles

Changes in the average size of particles were followed by the dependence of turbidity (τ) on wavelength (λ) of the suspensions, and determined as $\beta = 4.2 + \partial \log \tau / \partial \log \lambda$. β is a parameter that has a direct relationship with the average size of the particles and can be used to easily detect and follow rapid size changes. It was obtained from the slope of $\log \tau$ vs $\log \lambda$ plots, in the 450–650 nm range, where the absorption owing to the protein chromophores is negligible allowing then to estimate τ as absorbance in 400–800 nm range (Camerini-Otero & Day, 1978). It has been shown that β , for a system of aggregating particles of the characteristics of caseinates tends, upon aggregation, towards an asymptotic value that can be considered as a fractal dimension (D_f) of the aggregates (Horne, 1987; Mancilla Canales, Hidalgo, Risso, & Alvarez, 2010; Risso, Relling, Armesto, Pires, & Gatti, 2007). τ was measured as absorbance using a Spekol 1200 spectrophotometer (Anaikjenlyta, Belgium), with a diode arrangement. Determinations of β were the average of at least duplicate measurements.

2.13. Evaluation of acid aggregation process

Kinetics of NaCAS or hydrolysates (5 mg g⁻¹) and NaCAS:hydrolysates mixtures (4:1) aggregation, induced by the acidification with GDL, was analyzed by measuring τ in the range of 450–650 nm, in a spectrophotometer with a thermostated cell. The amount of GDL added was calculated using the relation $R = \text{GDL mass fraction} / \text{NaCAS mass fraction}$. R used for all these experiments was 0.5, at temperature of 35 °C.

Acidification was initiated by the addition of solid GDL to 6 g of different samples. Absorption spectra (450–650 nm) and

absorbance at 650 nm (A_{650}) were registered as a function of time until a maximum and constant value of A_{650} was reached; simultaneously, pH decrease was measured. The determinations were performed in duplicate and the values of parameter β were calculated as above mentioned.

2.14. Rheological properties of NaCAS:hydrolysate mixtures

Gel formation of NaCAS:hydrolysate mixtures (30 mg g^{-1} : 7.5 mg g^{-1}) was evaluated by oscillatory measurements using a stress and strain controlled rheometer (TA Instruments, AR G2 model, Brookfield Engineering Laboratories, Middleboro, USA). A cone geometry (diameter: 40 mm, cone angle: 2° , cone truncation: 55 mm) and a system of temperature control with a recirculating bath (Julabo model ACW 100, Seelbach, Alemania) connected to a Peltier plate were used for the measurements. Solid GDL was added in order to initiate the acid gelation at $R = 0.5$. Measurements were performed every 20 s for 120 min with a constant oscillation stress of 0.1 Pa and a frequency of 0.1 Hz. The Lissajous figures at various times were plotted to make sure that the determinations of storage or elastic modulus (G') and loss or viscous modulus (G'') were always obtained within the linear viscoelastic region. The complex modulus (G^*) and the pH were also monitored during acid gelation. Measurements were performed at least in triplicate.

2.15. Confocal laser scanning microscopy (CSLM)

NaCAS:hydrolysate mixtures (30 mg g^{-1} : 7.5 mg g^{-1}) were stained with Rhodamine B solution ($2 \times 10^{-3} \text{ mg mL}^{-1}$). An adequate amount of GDL ($R = 0.5$) was added to initiate the gelation process. Aliquots of 200 μL were immediately placed in compartments of LAB-TEK II cells (Thermo Scientific, USA). The gelation process was performed in an oven at $(35 \pm 1)^\circ\text{C}$, keeping the humidity controlled. Gels were observed with an $40\times$ objective, a $2\times$ zoom, by using an inverted scan confocal microscope NIKON TE2000E (Nikon Instruments Inc., USA), with handheld scanning, using 543 nm excitation He-Ne laser, 605–675 nm band emission. Acquired images were stored in tiff format for their further analysis.

In order to process the images obtained by CSLM and to obtain the texture parameters, specific programs were developed in Python language. The following three texture measures were used in this work: Shannon entropy (S), smoothness (K) and uniformity (U), given by:

$$S = - \sum_{i=0}^{L-1} p(N_i) \log_2(p(N_i)) \quad U = \sum_{i=0}^{L-1} p^2(N_i) \quad K = 1 - \frac{1}{1 + \frac{\sigma^2(N)}{(L-1)^2}} \quad (1)$$

where $p(N_i)$ is the statistical sample frequency normalized from the grey scale, L is the highest black level and $\sigma^2(N)$ is the mean normalized grey-level variance which is particularly important in texture description because it is a measure of grey level contrast that may be used to establish descriptors of relative smoothness (Gonzalez & Woods, 2001). Previously, the color images were transformed into normalized grey scale (8-bit) to achieve maximum contrast. Also, the mean diameter and area of pores or interstices were determined through ImageJ software, according to Pugnali, Matia-Merino and Dickinson (Pugnali, Matia-Merino, & Dickinson, 2005). The effect of time of hydrolysis on both parameters was evaluated using a Mixed-Model Nested ANOVA Design ($p < 0.05$). A Tukey HSD test was performed to analyze the mean differences between the levels of the time factor of hydrolysis.

2.16. Statistical analysis

The data are reported as the average values \pm their standard deviations. Statistical analyses were performed with Sigma Plot v.10.0, Origin v.6.1 and Statgraph v.5.0 softwares. The relationship between variables was statistically analyzed by correlation analysis using Pearson correlation coefficient (p). The differences were considered statistically significant at $p < 0.05$ values.

3. Results and discussion

3.1. NaCAS hydrolysis by P7PP

P7PP displayed a proteolytic activity, as assayed by the azocasein method, of 70 U mL^{-1} ($1,600 \text{ U mg protein}^{-1}$). Hydrolysis of NaCAS with P7PP was carried out for up to 7 h and, during this period, the DH was determined in hydrolysate supernatants (Fig. 1). Although the DH reached 8.2% after 7 h, higher hydrolysis rates were observed in the first four hours of hydrolysis, where the DH approached 6.2% in t_4 , decreasing afterwards. Since the DH measures the number of cleaved peptide bonds, the slower rates of DH increase indicate the lesser availability of cleavable peptide in the protein substrate, a behavior that is governed by enzyme specificity. A similar DH profile was observed for bovine NaCAS hydrolysates obtained with *Bacillus* sp. P45 protease (Hidalgo et al., 2012). However, during ovine NaCAS hydrolysis with P7PP, the release of amino groups (or peptide bonds cleaved) was somewhat lower during the hydrolysis process, which might reflect substrate (caseins) heterogeneity across species (Minervini et al., 2003).

The results of peptide mass distribution confirmed that the highest proportion of molecular masses of the hydrolysates obtained until 4 h of hydrolysis were lower than 3,000 Da (Fig. 2). However, a little portion of peptides with molecular masses between 3,000 and 5,000 Da during the first hydrolysis times measured was observed (data not shown).

Peptides with a signal/noise ratio higher than 10 were fragmented and their sequences were studied. Four peptides with a small size between 10 and 20 amino acid residues were identified. Molecular masses of 1,140.67, 1,641.90, 1,788.96 and 2,107.23 Da correspond to the sequences RPKHPIKHQG, QGLPQEVLNENLLRFF, QGLPQEVLNENLLRFFV and FLLYQEPVLGPPVRGPFPIIV, respectively. These peptides constitute fractions of α_{S1} -CN (f1-10), α_{S1} -CN (f9-24), α_{S1} -CN (f9-25) and β -CN (f190-209), respectively.

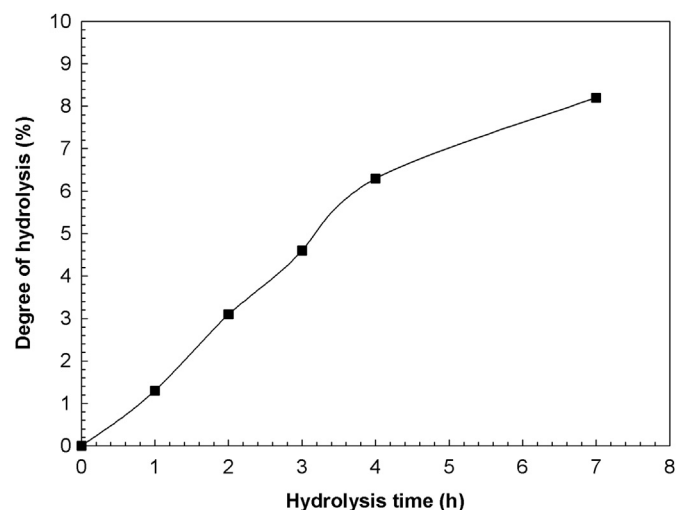


Fig. 1. Degree of hydrolysis (DH) of NaCAS obtained with a protease preparation from *Bacillus* sp. P7 (P7PP).

Among these peptides, two of them represented β -CN C-terminal and α_{S1} -CN N-initial fragments. On the other hand, in general, the P7PP cleavage occurred in the junction between two residues with nonpolar side chains, such as F-V, V-A, G-L, A-F. Although other authors have not reported the exact sequence of these peptides, different fragments of these sequences have been informed. Larsen et al. (2010) have reported the existence of peptides in the milk of cows previously infected with the mastitis virus, with similar sequences to those we have identified: α_{S1} -CN (f2-22), α_{S1} -CN (f8-21), β -CN (f199-209), β -CN (f192-209), β -CN (f193-209) (Larsen et al., 2010). Also, Bezerra (2011) identified three peptides employing a *Penicillium auratiogriseum* protease to hydrolyze caprine milk. These β -CN peptides presented similar sequences compared with those we obtained: β -CN (f191-207), β -CN (f194-202) and β -CN (f191-206). These authors reported that these β -CN fragments showed antioxidant activities *in vitro* (Bezerra, 2011). On the other hand, Andriamihaja et al. (2013) employed two microbial

enzymatic preparations from *Bacillus subtilis* and pancreatin with the aim of generating small, medium-size and large polypeptides from bovine CN during 2 h of hydrolysis. They have reported the presence of two peptides from β -CN and five from α_{S1} -CN, whose sequences, in some fragments, were consistent with those identified in our work: β -CN (f191-209), β -CN (f191-207), α_{S1} -CN (f1-13), α_{S1} -CN (f1-16), α_{S1} -CN (f1-15), α_{S1} -CN (f1-19), α_{S1} -CN (f1-20) (Andriamihaja et al., 2013). Finally, Kalyankar et al. (2013) reported the presence of three peptides from α_{S1} -CN (f1-18, f1-30, f3-30) using a glutamyl endopeptidase from Alcalase™ during 2 h of hydrolysis (Kalyankar, Zhu, O' Keeffe, O' Cuinn, & FitzGerald, 2013).

3.2. Intrinsic fluorescence spectra and surface hydrophobicity

Emission spectra of NaCAS and the hydrolysates obtained at different times of hydrolysis (t_i) are presented in Fig. 3.

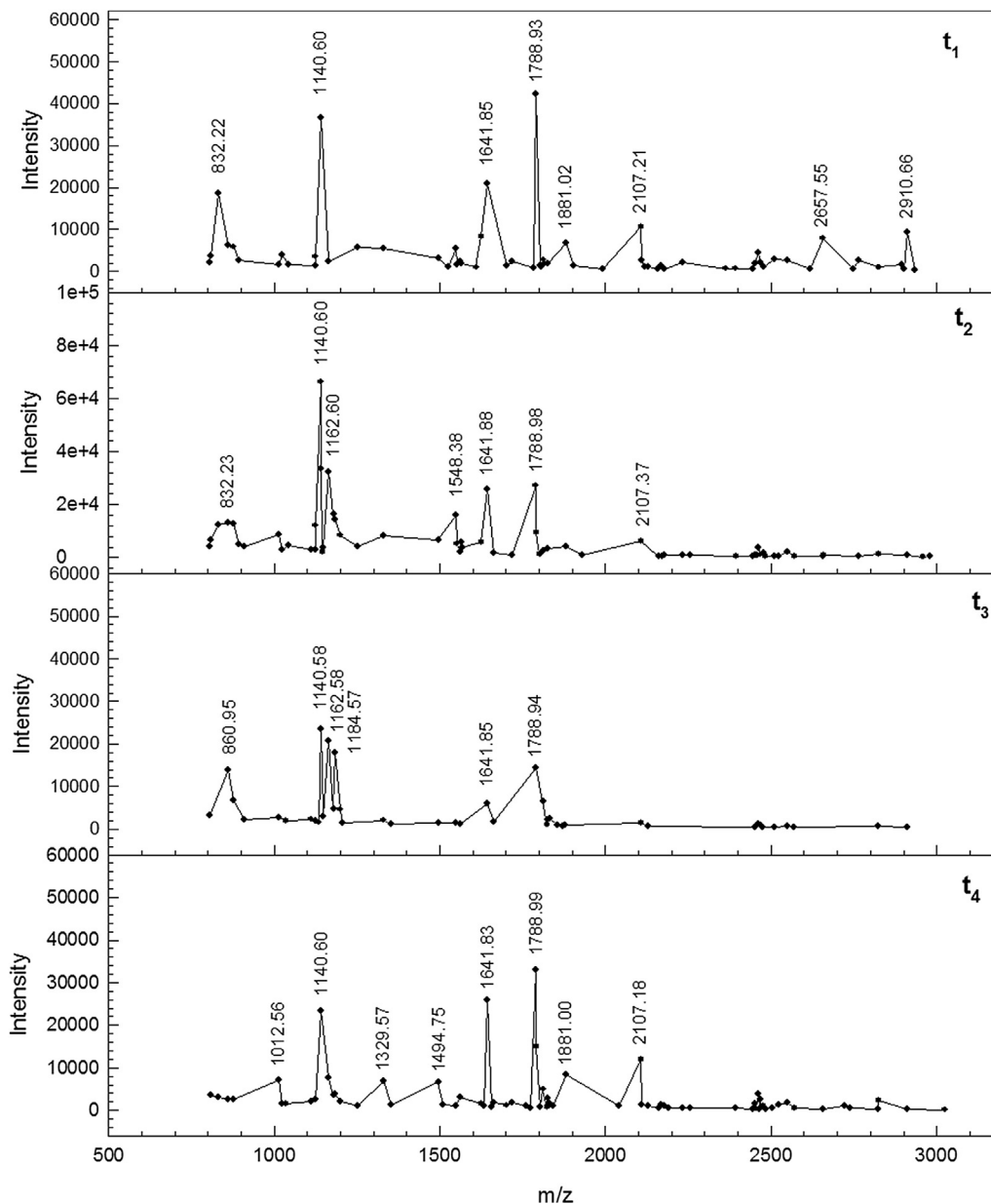


Fig. 2. Peptide mass distribution determined by MALDI-TOF-TOF mass spectrometry of hydrolysates obtained from NaCAS hydrolysis with P7PP for 1 (t_1), 2 (t_2), 3 (t_3) and 4 (t_4) hours.

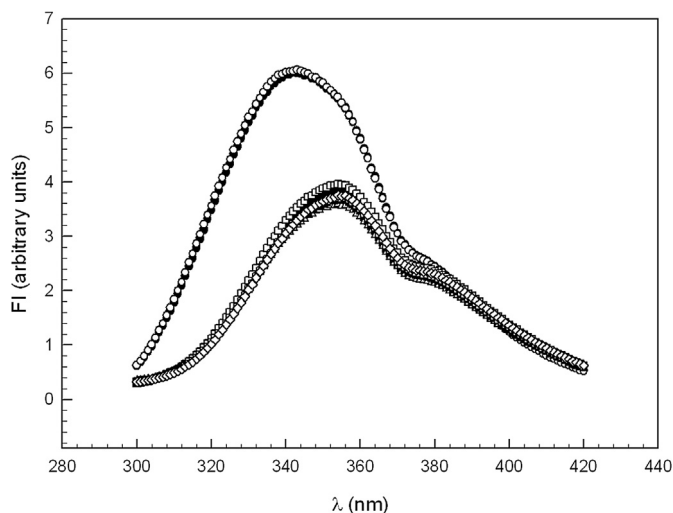


Fig. 3. Fluorescence emission spectra of the hydrolysates obtained through proteolysis with P7PP at different times (t_i): (●) NaCAS without hydrolysis; (○) t_0 ; (▲) t_1 ; (△) t_2 ; (■) t_3 ; (□) t_4 ; (◇) t_5 , where the subscript i correspond to the hydrolysis time. Hydrolysates concentration = 1 mg g^{-1} ; Range of λ_{em} = 300–420 nm, λ_{exc} 286 nm; T 35 °C.

Hydrolysis caused a fluorescence red shift as well as a decrease in the fluorescence intensity (FI), which might be due to conformational changes. These changes would indicate an increment of the polarity in the surroundings of intrinsic fluorophore groups in the peptides (Trp and Tyr). Previously, it was verified that during enzymatic proteolysis there was no loss of protein fluorophores occurs (data not shown).

S_0 ($\text{g}/100 \text{ g}^{-1}$) of NaCAS hydrolysates decreased as t_i increased (except for t_1): $t_0 = 111.2 \pm 0.2$, $t_1 = 170.1 \pm 0.2$, $t_2 = 83.4 \pm 0.2$, $t_3 = 31.4 \pm 0.3$. In the case of hydrolysate t_4 , S_0 values were not informed because these values are close to the experimental error. These results would indicate that after 1 h of hydrolysis, a higher exposure of hydrophobic groups occurs on the protein surface. However, the decrease of S_0 as t_i increased would indicate the disappearance of hydrophobic patches in the peptide structure.

3.3. Evaluation of hydrolysates bioactivities in vitro

3.3.1. Antioxidant activity

Peptides and protein hydrolysates, obtained from the proteolysis of various food proteins, are reported to possess antioxidant activities. Antioxidant activities might protect biological systems against damage related to oxidative stress in human disease conditions. These antioxidant peptides and hydrolysates might also be employed in preventing oxidation reactions (such as lipid peroxidation) that lead to deterioration of foods and foodstuffs (Hogan, Zhang, Li, Wang,

& Zhou, 2009; Zhang, Li, & Zhou, 2010). The antioxidant activities, including ABTS radical scavenging, reducing power and ferrous ion chelating ability of the hydrolysates were evaluated.

The radical ABTS^{•+} scavenging ability of hydrolysates increased, reaching a maximum at t_6 (Table 1). Although NaCAS also exhibits antioxidant activity, the increment of this activity as the hydrolysis time increases suggests that the proteolytic process contributes to the biological activity.

Megjás et al. reported that histidine may be considered as a strong metal chelator due to the presence of an imidazole ring (Megjás et al., 2008). According to the results, it would seem that hydrolysis increases the accessibility of the metal to the casein histidine groups. Therefore, these results indicate that the hydrolysis of NaCAS could be useful to increase mineral bioavailability. Also, NaCAS hydrolysates could be used as natural antioxidants to prevent oxidation reactions in the development of functional food products and additives.

Transition metals such as Fe^{2+} promote the lipid peroxidation and then their chelation helps to retard the peroxidation and prevent food rancidity (Zhang, Li, & Zhou, 2010). As observed in Table 1, NaCAS without hydrolysis presents iron chelation activity ($78.400 \pm 0.005\%$). This activity was significantly increased when the hydrolysis occur, reaching a maximum of $94.60 \pm 0.04\%$ at t_3 .

The reducing power assay is based on the capability of hydrolysates to reduce the Fe^{3+} /ferricyanide complex to the ferrous form. The results showed in Table 1 suggest that NaCAS hydrolysates would act as electron donors reducing the oxidized intermediates of lipidic peroxidation. The fact that the reducing power of the NaCAS hydrolysates is associated with this antioxidant activity suggested that the reducing power was likely to contribute significantly towards the observed antioxidant effect (Corrêa et al., 2011; Zhu et al., 2006). The reducing power of the hydrolysates reached a maximum value at t_3 and then diminished. According to mass spectrometry assays, the amount of small peptides increases as hydrolysis time increases. This suggests that the higher molecular mass of the hydrolysate, the higher reducing power activity. This behavior was also reported by other authors (Chang et al., 2007; Corrêa et al., 2011).

3.3.2. Antibacterial activity

The ability of NaCAS hydrolysates to inhibit the growth of many bacteria was then investigated. The results obtained are shown in Table 2.

Both Gram-positive and Gram-negative bacteria were inhibited but only the $t_{0.5}$ and t_1 hydrolysates inhibited the growth of *Salmonella Enteritidis*, *E. coli*, *C. fimi* and *L. monocytogenes*. These results are important because of these inhibited bacteria are important microorganisms related to foodborne diseases (Mor-Mur & Yuste, 2010). The antimicrobial activity observed for the NaCAS hydrolysates by the action of P7PP might represent a promising application to prevent the contamination of foods by these pathogenic microorganisms. Further interest is focused on caseins since these are safe food proteins abundantly available at low costs. Other authors have reported the identification of antibacterial domains within the sequence of bovine α_{S2} -CN (McCann et al., 2005; Recio & Visser, 1999), of α_{S1} -CN (McCann et al., 2006; Wu et al., 2013), of β -CN (Wu et al., 2013) and of κ -CN (Arruda et al., 2012). Particularly, Arruda et al. (2012) obtained fragments of α_{S1} -CN (f1-21, f1-23 and f8-23) and β -CN (f189-203) by casein hydrolysis during 2 h employing a new protease obtained from latex *Jacaratia corumbensis*. The sequence of these fragments, which partially coincides with α_{S1} -CN (f1-10, f9-24 and f9-25) and β -CN (f190-209) fragments previously reported in this work, demonstrate antibacterial activity against *Enterococcus faecalis*, *B. subtilis*, *E. coli*, *Pseudomonas aeruginosa*, *Klebsiella pneumonia* and *S. aureus* (Arruda et al., 2012).

Table 1

Antioxidant activities of the hydrolysates of NaCAS obtained by hydrolysis with P7PP.

Hydrolysis time (h)	ABTS radical scavenging activity (%)	Fe^{2+} -chelating ability (%)	Reducing power (absorbance at 700 nm)
0	52.60 ± 0.08^a	78.400 ± 0.005^a	0.106 ± 0.007^a
0.5	59.5 ± 0.1	89.800 ± 0.003	0.133 ± 0.002
1	70.20 ± 0.02	93.40 ± 0.02	0.171 ± 0.005
2	67.90 ± 0.05	93.300 ± 0.008	0.22 ± 0.03
3	71.20 ± 0.02	94.60 ± 0.04	0.30 ± 0.01
4	74.100 ± 0.008	80.300 ± 0.004	0.25 ± 0.01
6	75.30 ± 0.01	91.200 ± 0.005	0.262 ± 0.004

^a Mean value \pm standard deviation ($p < 0.05$).

Table 2
Antimicrobial activities of the hydrolysates obtained by hydrolysis of NaCAS with P7PP.

Indicator microorganism	Inhibition zone (mm) ^a	
Hydrolysis time (h)	0.5	1.0
Gram-positive bacteria		
<i>Listeria monocytogenes</i> ATCC 15131	8.0	10.0
<i>Bacillus cereus</i> ATCC 9634	– ^b	
<i>Corynebacterium fimi</i> NCTC 7547	7.0	10.0
<i>Staphylococcus aureus</i> ATCC 1901	–	
Gram-negative bacteria		
<i>Salmonella enteritidis</i> ATCC 13076	8.0	11.0
<i>Escherichia coli</i> ATCC 8739	6.0	9.0

^a Values for haloes are the means of three independent determinations.

^b Without inhibition.

The higher susceptibility of Gram-positive microorganisms to casein-derived peptides, when compared to Gram-negative bacteria, might be attributed to the more complex cellular envelope of the latter (López-Expósito, Gómez-Ruiz, Amigo, & Recio, 2006).

3.4. Acid aggregation of NaCAS hydrolysates

The acid aggregation of NaCAS hydrolysates was evaluated by the variations of $A_{650\text{nm}}$ as a function of time (Fig. 4A). The results show that the hydrolysates did not maintain the capability to aggregate, except for t_0 , which is the sample that was not hydrolyzed (control). The absence of formation of aggregates from t_{1-7} hydrolysates, detectable by this technique, is probably due to the small average size of the particles that do not form aggregates or generate a small aggregates (smaller than the incident λ) not detected by turbidity measurements.

On the other hand, no changes on the rate at which pH becomes lower were detected (Fig. 4B).

3.5. Acid aggregation of NaCAS:hydrolysates mixtures

With the aim of evaluating whether the addition of the hydrolysates with biological activities modifies the kinetics of NaCAS aggregation and/or the degree of compactness of the aggregate formed, acid aggregation of NaCAS:hydrolysates mixtures (4:1) was evaluated analyzing how parameter β is modified as a function of time and pH after adding GDL (Fig. 5).

The aggregation process observed was similar to those previously reported for non-hydrolyzed bovine NaCAS and reveals two

well-defined steps (Hidalgo et al., 2011). At the first aggregation stage, the decrease in the average diameters, estimated by β values, may be due to a dissociation of pre-existing aggregates along together with the formation of a large amount of new aggregates of smaller size due to a loss of the net charge of the particles, which reduces their electrostatic stability and makes them more susceptible to flocculation. At pH values near the isoelectric point, the higher number of particles with electrostatic destabilization causes the formation of much larger particle size aggregates.

In presence of hydrolysates, changes in the time at which the second step starts (t_{ag}) were observed (increment of t_{ag}) but the pH value observed at t_{ag} (pH_{ag}) was shown to be similar to that of non-hydrolyzed NaCAS. There were also no changes on the rate at which the pH becomes lower. These results indicate that the electrostatic stability of NaCAS is not appreciably affected by the presence of hydrolysates.

On the other hand, the decrease of superficial hydrophobic residues as hydrolysis time increases (estimated by S_0 values), the probability of hydrophobic interactions between destabilized particles diminishes. Therefore, as hydrolysis time increases, the time at which the aggregates formation starts is higher.

As from the estimation of the fractal dimension by turbidimetry, no significant changes were observed in the degree of compactness of the aggregates (D_f) formed at the end of the acidification process of NaCAS:hydrolysate mixtures at low concentrations (Table 3).

Taking into account these results, it is important to assess the behavior of these mixtures at concentrations at which the decrease in pH leads to the formation of acid gels. Therefore, the rheological behavior and the microstructure of such gels were evaluated.

3.6. Rheological behavior of NaCAS:hydrolysate mixtures

Aiming at studying the effect of the presence of the hydrolysates on NaCAS gelation, the acid gelation process of NaCAS:hydrolysate mixtures was studied. Previously, it was found that the hydrolysates did not form acid gels after adding GDL. From the G' and G'' vs. time plots, the gel point was determined as the time when the G' and G'' crossover (t_g) occurred (Curcio et al., 2001). pH at t_g was also determined considering the pH value at the G' and G'' crossover (pH_g). Both t_g and pH_g showed no significant changes at all t_i assayed ($i = 0-4$) (data not shown). After gel point, G' and G'' increased up to a steady-state, G' being higher than G'' in all cases. Fig. 6 shows the variation of the complex shear modulus (G^*) vs. acidification time. Differences among the gels produced in the

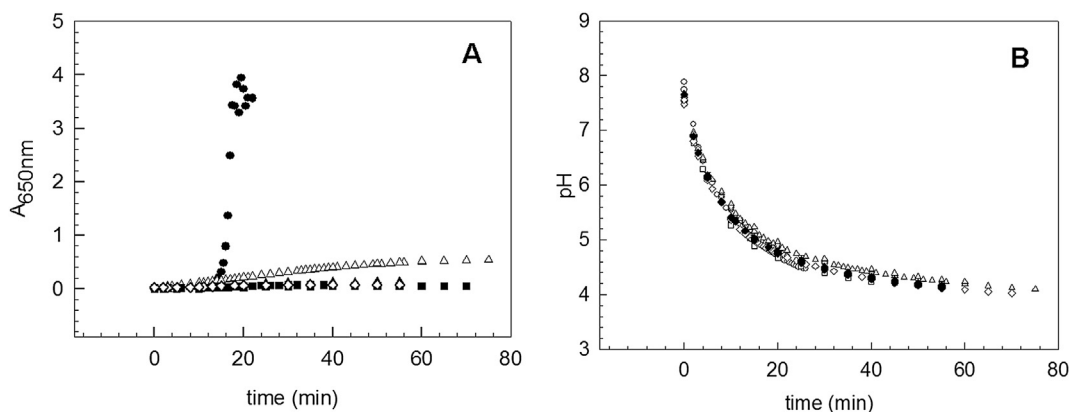


Fig. 4. Variations of the absorbance at 650 nm ($A_{650\text{nm}}$) (A) and pH (B) as a function of time, after glucono- δ -lactone (GDL) addition, during the acid aggregation of NaCAS hydrolysates t_0 (\bullet), t_1 (Δ), t_2 (\blacktriangle), t_3 (\square), t_4 (\blacksquare), and t_7 (\diamond), where the subscript i correspond to the hydrolysis time. Assays performed at 35 °C; GDL mass fraction/protein mass fraction (R) = 0.5; hydrolysates concentration = 5 mg g⁻¹.

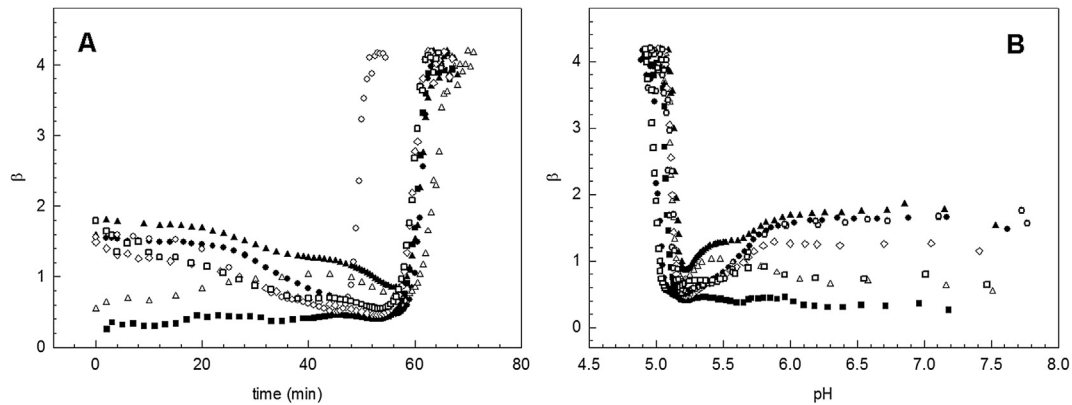


Fig. 5. Variations of parameter β , proportional to the average size of particles, as a function of time (A) and pH (B), after glucono- δ -lactone (GDL) addition, during the acid aggregation of NaCAS:hydrolysates mixtures (4:1): NaCAS without hydrolysate (\circ), with t_0 (\bullet), with t_1 (Δ), with t_2 (\blacktriangle), with t_3 (\square), with t_4 (\blacksquare), and with t_7 (\diamond), where the subscript i correspond to the hydrolysis time. Assays performed at 35 °C; GDL mass fraction/protein mass fraction (R) = 0.5; NaCAS:hydrolysates total concentration = 5 mg g⁻¹.

Table 3

Values of fractal dimension (D_f) of NaCAS:hydrolysates mixtures (4:1), t_i = hydrolysis time (h). NaCAS concentration 5 mg mL⁻¹, hydrolysates concentration 1.25 mg mL⁻¹, GDL mass fraction/protein mass fraction (R) 0.5 and T 35 °C.

System	$D_f \pm 0.02^a$
NaCAS without hydrolysis	4.17
NaCAS: t_0	4.14
NaCAS: t_1	4.16
NaCAS: t_2	4.18
NaCAS: t_3	4.17
NaCAS: t_4	4.18

^a Mean value \pm standard deviation ($p < 0.05$).

presence of hydrolysates at the beginning of the gelation process can be observed.

The non-linear least-square regression method was used to fit the raw mechanical properties data as a function of acidification time:

$$G^* = G_{eq}^* + Ce^{-kt} \quad (2)$$

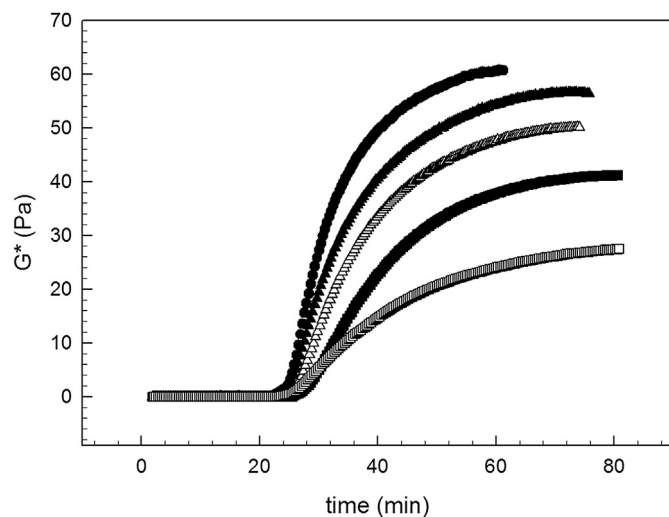


Fig. 6. Time dependence of the complex modulus G^* (at 0.1 Hz) for NaCAS:hydrolysates mixtures (4:1) acid gels obtained at different hydrolysis times (t_i): NaCAS:hydrolysate t_i : t_0 (\bullet), t_1 (Δ), t_2 (\blacktriangle), t_3 (\square), t_4 (\blacksquare), where the subscript i correspond to the hydrolysis time. NaCAS concentration: 30 mg g⁻¹, hydrolysate concentration: 7.5 mg g⁻¹, R = 0.5 and T = 35 °C.

where G_{eq}^* is the steady-state G^* value, k is the initial rate of increase in G^* , t is the time after GDL addition and C is a fitting parameter (Cavallieri & da Cunha, 2008). The values of G_{eq}^* and k are shown in Table 4.

At the beginning of gelation, the increase in G^* could reflect the increased contact between the NaCAS particles mediated by particle fusion, and subsequent interparticle rearrangements due to bond reversibility, which result in more bonds per junction and in more junctions, which in turn increases the storage modulus (Mellema, Walstra, van Opheusden, & van Vliet, 2002). According to our results, G_{eq}^* and k diminish in the presence of hydrolysates obtained at higher t_i , especially for hydrolysate t_4 . Therefore, the presence of hydrolysates would make the interparticle rearrangements difficult leading to a decrease of elastic character of gels.

3.7. Evaluation of gel microstructure

Fig. 7 shows representative microscopic images of NaCAS:hydrolysate t_0 and NaCAS:hydrolysate t_4 gels which were captured using CLSM. These images provide visual information regarding how the presence of hydrolysates affects the microstructure of NaCAS gels. Red pixels in the images are due to polypeptide chains dyed with Rhodamine B, while the black pixels are due to interstices formed. The CLSM images show a porous stranded network structure.

A comparison of both images indicates that the NaCAS gel network depends on the presence of hydrolysates. The pores around the polypeptide network become smaller with the increase in t_i (Table 5). Also, the pore diameter distribution indicates that the amount of smaller interstices was the highest for NaCAS:hydrolysate t_4 gels (Fig. 8). Therefore, as t_i increases, the amount of pores increases and these pores are even smaller.

Table 4

The steady-state value of the complex shear modulus (G_{eq}^*) and the initial rate of increase in G^* (k) for NaCAS:hydrolysates mixtures acid gels (4:1) obtained at different hydrolysis times (t_i). NaCAS concentration: 30 mg g⁻¹, hydrolysates concentration: 7.5 mg g⁻¹, R = 0.5 and T = 35 °C.

t_i	G_{eq}^* (Pa)	k (min ⁻¹)
t_0	61.4 \pm 0.1 ^a	0.1105 \pm 0.0008 ^a
t_1	57.60 \pm 0.08	0.0809 \pm 0.0005
t_2	51.59 \pm 0.04	0.0751 \pm 0.0002
t_3	43.16 \pm 0.08	0.0645 \pm 0.0004
t_4	29.56 \pm 0.04	0.0488 \pm 0.0002

^a Mean value \pm standard deviation ($p < 0.05$).

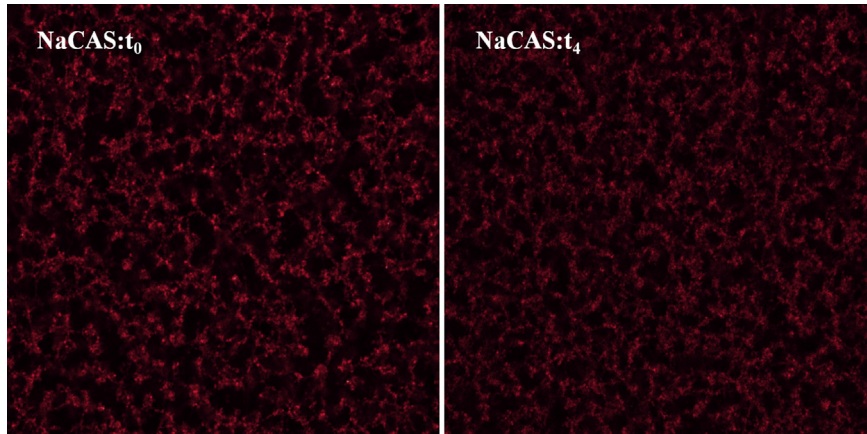


Fig. 7. Microphotographs of NaCAS:hydrolysates t_0 and t_4 gels obtained by CLSM, using Rhodamine B (2×10^{-3} mg mL $^{-1}$). NaCAS concentration: 30 mg g $^{-1}$, hydrolysate concentration: 7.5 mg g $^{-1}$, $R = 0.5$ and $T = 35$ °C.

Table 5

Mean pore diameters and pore area of acid gels obtained from NaCAS:hydrolysates t_i mixtures (30 mg g $^{-1}$:7.5 mg g $^{-1}$), where t_i is the hydrolysis time. Ratio GDL/NaCAS concentrations (R) = 0.5 and $T = 35$ °C.

NaCAS: hydrolysates t_i mixtures	Mean pore diameter ^a (μm)	Pore area ^a (μm)	Homogeneous group ^b
t_0	1.659 ± 0.021	3.519 ± 0.109	BC
t_1	1.733 ± 0.035	4.027 ± 0.211	C
t_2	1.678 ± 0.025	3.750 ± 0.138	BC
t_3	1.591 ± 0.023	3.334 ± 0.126	AB
t_4	1.521 ± 0.014	2.862 ± 0.083	A

^a Mean value ± standard deviation ($p < 0.05$).

^b Different letters denote mean value of mean pore diameter and pore area parameters significantly different among the values of t_i (A stands for the lowest, B for medium value and C for the highest value, respectively).

On the other hand, from the analysis of textural parameters (Table 6), we could conclude that the presence of hydrolysates (t_{1-4}) increases S and decreases U values. According to U values, t_0 image is smoother (more uniform) than t_4 image; i.e., microstructure for NaCAS:hydrolysate t_4 gel is more disordered. S values lead us to the same conclusion; t_0 image has the lowest variation in grey level. Therefore, the presence of hydrolysates (t_{1-4}) would make the ordered structure of NaCAS gels weaker. This observation is consistent with the lower value of G^* of these mixed gels (Fig. 6).

4. Conclusions

This study shows that a protease preparation from *Bacillus* sp. P7 could be used in the hydrolysis of bovine NaCAS to obtain peptides possessing different antioxidant and antimicrobial activities. Some

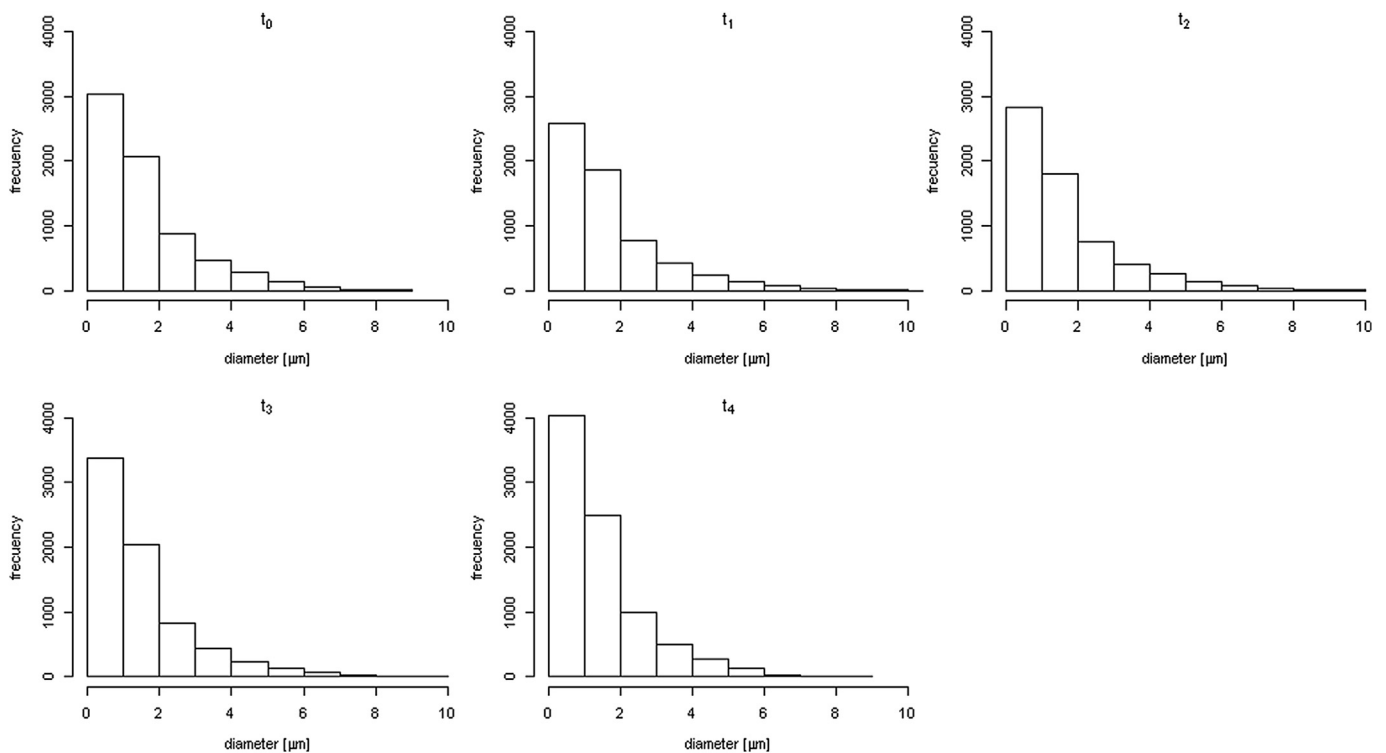


Fig. 8. Pore diameter distribution of NaCAS:hydrolysates gels obtained by addition of GDL at 35 °C. NaCAS concentration: 30 mg g $^{-1}$, hydrolysate concentration: 7.5 mg g $^{-1}$, $R = 0.5$.

Table 6

Textural parameters obtained from digital images of NaCAS:hydrolysate acid gels in function of hydrolysis time (t_i): Shannon entropy (S), smoothness (K), uniformity (U), and mean normalized grey-level variance ($\sigma^2(N)$). NaCAS concentration: 30 mg g⁻¹, hydrolysate concentration: 7.5 mg g⁻¹, $R = 0.5$ and $T = 35^\circ\text{C}$.

t_i	S	$K (\times 10^{-3})$	$U (\times 10^{-3})$	$\sigma^2(N)$	ANOVA for S	ANOVA for K	ANOVA for U	ANOVA for $\sigma^2(N)$
t_0	5.02 ± 0.03 ^d	3.67 ± 0.17	39.43 ± 0.97	239.48 ± 10.93	A ^b	A	C	A
t_1	5.26 ± 0.02	4.76 ± 0.12	32.95 ± 0.48	310.80 ± 7.82	B	C	B	AB
t_2	5.24 ± 0.03	4.43 ± 0.22	32.81 ± 0.70	289.04 ± 14.38	B	BC	B	AB
t_3	5.43 ± 0.04	4.97 ± 0.26	27.96 ± 0.88	325.04 ± 17.22	B	C	A	B
t_4	5.29 ± 0.02	4.09 ± 0.09	30.20 ± 0.40	266.95 ± 6.02	B	AB	AB	AB

^a Mean value ± standard deviation ($p < 0.05$).

^b Different letters denote mean value of parameter K , S , U , $\sigma^2(N)$ significantly different among the values of t_i (A stands for the lowest, B for medium value and C for the highest value, respectively).

of these peptides are fractions of α_{S1} -CN and β -CN, and parts of their sequences, with antioxidant and antibacterial activities, have been previously reported. The isolation of such bioactive peptides will be studied in further work.

The hydrolysates did not maintain the capability to aggregate under acid conditions when GDL was added. However, their incorporation in NaCAS solutions modifies the kinetics of the acid aggregation process but does not significantly alter the degree of compactness of the aggregate formed at low NaCAS concentration. On the other hand, at NaCAS concentrations where the decrease in pH leads to the formation of acid gels, the presence of hydrolysates leads to more porous and weaker gels, especially in the presence of hydrolysate t_4 . Therefore, these results suggest that these bioactive peptides modify the microstructure and rheological behavior when they are added into NaCAS acid gels.

Acknowledgements

This work was supported by grants from the Universidad Nacional de Rosario, Agencia Nacional de Promoción Científica y Tecnológica (PICT 2011 1354), the Cooperation Program between Coordenação de Aperfeiçoamento de Pessoal de Nível Superior (CAPES) from Brazil and the Ministerio de Ciencia, Tecnología e Innovación Productiva (MINCYT) from Argentina). Thanks to María Robson, Mariana de Sanctis and Geraldine Raimundo, for the English revision, to Bibiana Riquelme for image analysis, to Hebe Bottai for statistical analysis and to Silvia Moreno, María Pía Valacco and Ricardo Neme Tauli, from the CEQUIBIEM, for the mass spectrometry service.

References

- Adler-Nissen, J. (1979). Determination of the degree of hydrolysis of food protein hydrolysates by trinitrobenzenesulfonic acid. *Journal of Agricultural and Food Chemistry*, 27(6), 1256–1262.
- Alvarez, E., Risso, P., Gatti, C., Burgos, M., & Suarez Sala, V. (2007). Calcium-induced aggregation of bovine caseins: effect of phosphate and citrate. *Colloid & Polymer Science*, 285(5), 507–514.
- Andriamihaja, M., Guillot, A., Svendsen, A., Hagedorn, J., Rakotondratohanina, S., Tomé, D., et al. (2013). Comparative efficiency of microbial enzyme preparations versus pancreatin for in vitro alimentary protein digestion. *Amino Acids*, 44(2), 563–572.
- Arruda, M. S., Silva, F. O., Egito, A. S., Silva, T. M. S., Lima-Filho, J. L., Porto, A. L. F., et al. (2012). New peptides obtained by hydrolysis of caseins from bovine milk by protease extracted from the latex *Jacaratia corumbensis*. *LWT - Food Science and Technology*, 49(1), 73–79.
- Bezerra, V. S. (2011). *Caracterização e atividade biológica de peptídeos obtidos pela hidrólise enzimática de caseína do leite de cabra Moxotó (Capra hircus Linnaeus, 1758)*. Recife: Universidade Federal Rural de Pernambuco. Unpublished Doutorado em Biociência Animal.
- Braga, A. L. M., Menossi, M., & Cunha, R. L. (2006). The effect of the glucono-[delta]-lactone/caseinate ratio on sodium caseinate gelation. *International Dairy Journal*, 16(5), 389–398.
- Camerini-Otero, R. D., & Day, L. A. (1978). The wavelength dependence of the turbidity of solutions of macromolecules. *Biopolymers*, 17(9), 2241–2249.
- Cavallieri, A. L. F., & da Cunha, R. L. (2008). The effects of acidification rate, pH and ageing time on the acidic cold set gelation of whey proteins. *Food Hydrocolloids*, 22(3), 439–448.
- Chang, C.-Y., Wu, K.-C., & Chiang, S.-H. (2007). Antioxidant properties and protein compositions of porcine haemoglobin hydrolysates. *Food Chemistry*, 100(4), 1537–1543.
- Corrêa, A. P. F., Daroit, D. J., & Brandelli, A. (2010). Characterization of a keratinase produced by *Bacillus* sp. P7 isolated from an Amazonian environment. *International Biodeterioration & Biodegradation*, 64(1), 1–6.
- Corrêa, A. P. F., Daroit, D. J., Coelho, J., Meira, S. M. M., Lopes, F. C., Segalin, J., et al. (2011). Antioxidant, antihypertensive and antimicrobial properties of ovine milk caseinate hydrolyzed with a microbial protease. *Journal of the Science of Food and Agriculture*, 91(12), 2247–2254.
- Corzo-Martínez, M., Moreno, F. J., Villamiel, M., & Harte, F. M. (2010). Characterization and improvement of rheological properties of sodium caseinate glycated with galactose, lactose and dextran. *Food Hydrocolloids*, 24(1), 88–97.
- Curcio, S., Gabriele, D., Giordano, V., Calabrò, V., de Cindio, B., & Iorio, G. (2001). A rheological approach to the study of concentrated milk clotting. *Rheologica Acta*, 40(2), 154–161.
- FitzGerald, R. J., Murray, B. A., & Walsh, D. J. (2004). Hypotensive peptides from milk proteins. *Journal of Nutrition*, 134(4), 980S–988S.
- Gonzalez, J., & Woods, R. E. (2001). *Digital image processing* (2nd ed.). Prentice Hall.
- Gupta, R., Beg, Q. K., & Lorenz, P. (2002). Bacterial alkaline proteases: molecular approaches and industrial applications. *Applied Microbiology and Biotechnology*, 59(1), 15–32.
- Haque, E., & Chand, R. (2008). Antihypertensive and antimicrobial bioactive peptides from milk proteins. *European Food Research and Technology*, 227(1), 7–15.
- Hartmann, R., & Meisel, H. (2007). Food-derived peptides with biological activity: from research to food applications. *Current Opinion in Biotechnology*, 18(2), 163–169.
- Hidalgo, M. E., Daroit, D. J., Folmer Corrêa, A. P., Pieniz, S., Brandelli, A., & Risso, P. H. (2012). Physicochemical and antioxidant properties of bovine caseinate hydrolysates obtained through microbial protease treatment. *International Journal of Dairy Technology*, 65(3), 342–352.
- Hidalgo, M. E., Mancilla Canales, M. A., Nespolo, C. R., Reggiardo, A. D., Alvarez, E. M., Wagner, J. R., et al. (2011). Comparative study of bovine and ovine caseinate aggregation processes: calcium-induced aggregation and acid aggregation. In D. A. Stein (Ed.), *Protein aggregation* (pp. 199–222). Hauppauge, NY: Nova Publishers.
- Hogan, S., Zhang, L., Li, J., Wang, H., & Zhou, K. (2009). Development of antioxidant rich peptides from milk protein by microbial proteases and analysis of their effects on lipid peroxidation in cooked beef. *Food Chemistry*, 117, 438–443.
- Horne, D. S. (1987). Determination of the fractal dimension using turbidimetric techniques. Application to aggregating protein systems. *Faraday Discussions of the Chemical Society*, 83(0), 259–270.
- Kalyankar, P., Zhu, Y., O'Keeffe, M., O'Cuinn, G., & FitzGerald, R. J. (2013). Substrate specificity of glutamyl endopeptidase (GE): hydrolysis studies with a bovine α -casein preparation. *Food Chemistry*, 136(2), 501–512.
- Kato, A., & Nakai, S. (1980). Hydrophobicity determined by a fluorescence probe method and its correlation with surface properties of proteins. *Biochimica et Biophysica Acta (BBA) - Protein Structure*, 624(1), 13–20.
- Korhonen, H. (2009). Milk-derived bioactive peptides: from science to applications. *Journal of Functional Foods*, 1, 177–187.
- de Kruijf, C. G. (1997). Skim milk acidification. *Journal of Colloid and Interface Science*, 185(1), 19–25.
- Kuaye, A. Y. (1994). An ultraviolet spectrophotometric method to determine milk protein content in alkaline medium. *Food Chemistry*, 49(2), 207–211.
- Larsen, L. B., Hinz, K., Jørgensen, A. L. W., Møller, H. S., Wellnitz, O., Bruckmaier, R. M., et al. (2010). Proteomic and peptidomic study of proteolysis in quarter milk after infusion with lipoteichoic acid from *Staphylococcus aureus*. *Journal of Dairy Science*, 93(12), 5613–5626.
- Li, B., Chen, F., Wang, X., Ji, B., & Wu, Y. (2007). Isolation and identification of antioxidative peptides from porcine collagen hydrolysate by consecutive chromatography and electrospray ionization-mass spectrometry. *Food Chemistry*, 102(4), 1135–1143.
- López-Expósito, I., Gómez-Ruiz, J., Amigo, L., & Recio, I. (2006). Identification of antibacterial peptides from ovine α 2-casein. *International Dairy Journal*, 16, 1072–1080.
- Mancilla Canales, M. A., Hidalgo, M. E., Risso, P. H., & Alvarez, E. M. (2010). Colloidal stability of bovine calcium caseinate suspensions. Effect of protein concentration and the presence of sucrose and lactose. *Journal of Chemical & Engineering Data*, 55(7), 2550–2557.

- McCann, K. B., Shiell, B. J., Michalski, W. P., Lee, A., Wan, J., Roginski, H., et al. (2005). Isolation and characterisation of antibacterial peptides derived from the f(164–207) region of bovine α S2-casein. *International Dairy Journal*, 15(2), 133–143.
- McCann, K. B., Shiell, B. J., Michalski, W. P., Lee, A., Wan, J., Roginski, H., et al. (2006). Isolation and characterisation of a novel antibacterial peptide from bovine α S1-casein. *International Dairy Journal*, 16(4), 316–323.
- Megias, C., Pedroche, J., Yust, M. M., Girón-Calle, J., Alaiz, M., Millán, F., et al. (2008). Production of copper-chelating peptides after hydrolysis of sunflower proteins with pepsin and pancreatin. *LWT - Food Science and Technology*, 41(10), 1973–1977.
- Mellema, M., Walstra, P., van Opheusden, J. H., & van Vliet, T. (2002). Effects of structural rearrangements on the rheology of rennet-induced casein particle gels. *Advances in Colloid and Interface Science*, 98(1), 25–50.
- Minervini, F., Algaron, F., Rizzello, C. G., Fox, P. F., Monnet, V., & Gobetti, M. (2003). Angiotensin I-converting-enzyme-inhibitory and antibacterial peptides from *Lactobacillus helveticus* PR4 proteinase-hydrolyzed caseins of milk from six species. *Applied and Environmental Microbiology*, 69(9), 5297–5305.
- Mor-Mur, M., & Yuste, J. (2010). Emerging bacterial pathogens in meat and poultry: an overview. *Food Bioprocess Technology*, 3, 24–35.
- Motta, A., & Brandelli, A. (2002). Characterization of an antibacterial peptide produced by *Brevibacterium linens*. *Journal of Applied Microbiology*, 92(1), 63–70.
- Mulvihill, D. M., & Fox, P. F. (1989). Caseins and manufactured. In P. F. Fox (Ed.), *Development in dairy chemistry* (vol. 4, pp. 97–130). London & New York: Elsevier Applied Science.
- Nishinari, K., Zhang, H., & Ikeda, S. (2000). Hydrocolloid gels of polysaccharides and proteins. *Current Opinion in Colloid & Interface Science*, 5(3–4), 195–201.
- Phelan, M., Aherne, A., FitzGerald, R. J., & O'Brien, N. M. (2009). Casein-derived bioactive peptides: biological effects, industrial uses, safety aspects and regulatory status. *International Dairy Journal*, 19(11), 643–654.
- Pugnaloni, L. A., Matia-Merino, L., & Dickinson, E. (2005). Microstructure of acid-induced caseinate gels containing sucrose: quantification from confocal microscopy and image analysis. *Colloids and Surfaces B: Biointerfaces*, 42(3–4), 211–217.
- Rabiey, L., & Britten, M. (2009). Effect of whey protein enzymatic hydrolysis on the rheological properties of acid-induced gels. *Food Hydrocolloids*, 23(8), 2302–2308.
- Rao, M. B., Tanksale, A. M., Ghatge, M. S., & Deshpande, V. V. (1998). Molecular and biotechnological aspects of microbial proteases. *Microbiology and Molecular Biology Reviews*, 62(3), 597–635.
- Re, R., Pellegrini, N., Proteggente, A., Pannala, A., Yang, M., & Rice-Evans, C. (1999). Antioxidant activity applying an improved ABTS radical cation decolorization assay. *Free Radic BiolMed*, 26, 1231–1237.
- Recio, I., & Visser, S. (1999). Identification of two distinct antibacterial domains within the sequence of bovine α S2-casein. *Biochimica et Biophysica Acta (BBA) – General Subjects*, 1428(2–3), 314–326.
- Risso, P., Relling, V., Armesto, M., Pires, M., & Gatti, C. (2007). Effect of size, proteic composition, and heat treatment on the colloidal stability of proteolyzed bovine casein micelles. *Colloid & Polymer Science*, 285(7), 809–817.
- Rival, S. G., Boeriu, C. G., & Wichers, H. J. (2001). Caseins and casein hydrolysates. 2. Antioxidative properties and relevance to lipoxigenase inhibition. *Journal of Agricultural and Food Chemistry*, 49, 295–302.
- Saiga, A., Tanabe, S., & Nishimiura, T. (2003). Antioxidant activity of peptides obtained from porcine myofibrillar proteins by protease treatment. *Journal of Agricultural and Food Chemistry*, 51, 3661–3667.
- Sarmadi, B. H., & Ismail, A. (2010). Antioxidative peptides from food proteins: a review. *Peptides*, 31(10), 1949–1956.
- Silva, S. V., & Malcata, F. X. (2005). Caseins as source of bioactive peptides. *International Dairy Journal*, 15(1), 1–15.
- Walstra, P., Jenness, R., & Badings, H. T. (1984). *Dairy chemistry and physics*. New York, USA: John Wiley & Sons.
- Wu, S., Qi, W., Li, T., Lu, D., Su, R., & He, Z. (2013). Simultaneous production of multi-functional peptides by pancreatic hydrolysis of bovine casein in an enzymatic membrane reactor via combinational chromatography. *Food Chemistry*, 141(3), 2944–2951.
- Zhang, L., Li, J., & Zhou, K. (2010). Chelating and radical scavenging activities of soy protein hydrolysates prepared from microbial proteases and their effect on meat lipid peroxidation. *Bioresource Technology*, 101(7), 2084–2089.
- Zhu, K., Zhou, H., & Qian, H. (2006). Antioxidant and free radical-scavenging activities of wheat germ protein hydrolysates (WGPH) prepared with alcalase. *Process Biochemistry*, 41(6), 1296–1302.